Estimation of Equivalent Thermal Conductivity for Impregnated Electrical Windings Formed from Profiled Rectangular Conductors

S Ayat*†, R Wrobel*†, J Goss†, D Drury*

** Department of Electrical and Electronic Engineering, University of Bristol, Bristol, UK,*
s.ayat@bristol.ac.uk, r.wrobel@bristol.ac.uk, d.drury@bristol.ac.uk
† Motor Design Ltd. Ellesmere, UK, james.goss@motor-design.com

Keywords: Winding homogenisation techniques, equivalent thermal properties, thermal analysis, electrical machines.

Abstract

In order to improve accuracy and reduce model setting-up and solving time in thermal analysis of electrical machines, transformers and wound passive components, the multi-material winding region is frequently homogenised. The existing winding homogenization techniques are predominantly focused on winding constructions with round conductors, where thermal conductivity across conductors is usually assumed to be isotropic. However, for the profiled rectangular conductors that assumption is no longer valid, and anisotropy of the winding equivalent thermal conductivity needs to be considered.

This paper presents analytical methods for deriving equivalent thermal properties of impregnated windings with profiled rectangular conductors. The techniques allow for computationally efficient and accurate derivation of the composite thermal conductivity accounting for the material thermal anisotropy. Efficacy of the methods has been demonstrated on a number of hardware winding samples commonly used in low-voltage applications. The theoretical analysis has been supplemented with experimentally derived data showing close correlation.

1 Introduction

The winding region is frequently attributed with the dominant power loss source within an electrical machine assembly. A well-informed design process of the winding assembly is therefore prerequisite of compact, high-power-density and/or high-efficiency machine solutions. An electrical winding designed for the low-voltage applications is a composite structure formed from conductors coated with an appropriate grade of electrical insulation commonly referred to as enamel. The complete winding assembly is usually impregnated with varnish or epoxy resin to further improve the electrical insulation and provide 'good' heat transfer from the winding body into the machine periphery, and also assure mechanical rigidity and robustness.

The winding assembly is prone to numerous air pockets and/or cavities resulting from the winding arrangement, impregnating material and manufacture process used among others.

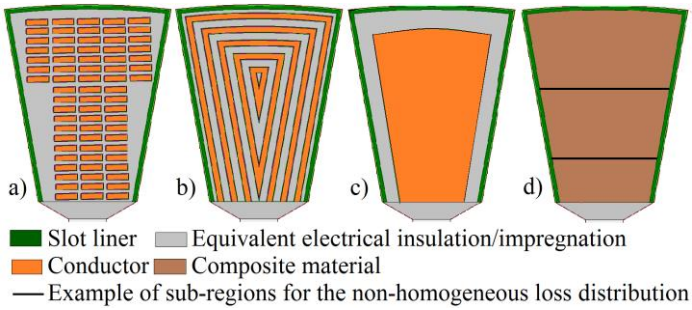

Figure 1: Schematic cross-section of a stator slot with alternative winding representations used in thermal analysis of electrical machines: a) physical model, b) layered model, c) equivalent material model, d) homogenised model

These manufacture and assembly imperfections/nuances have been shown to have a significant influence on the winding equivalent thermal conductivity making the accurate estimation of the winding thermal properties challenging for a machine designer [1, 2].

The computational methods employed in thermal analysis of electrical machines, transformers and wound passive components make use of various techniques for representing the winding region. The existing methods have been schematically shown in Fig. 1. The level of complexity for the winding model representation is usually chosen based on required fidelity for the temperature predictions within the machine assembly. This is driven by numerous factors, some of which include: the power loss sources and mechanisms accounted for, e.g. inhomogeneous loss distribution in the machine active regions [3]-[5]; higher resolution for the temperature predictions, e.g. accurate identification of the hot-spots [5]-[8]; reduced computational effort, e.g. thermal envelope mapping for a given operating envelope and/or cycle.

The physical representation of winding region with the individual winding conductors accounted for, Fig. 1a), is the most intuitive among the existing alternatives. However, the setting-up and solving time for such defined thermal model is frequently prohibitively high as all the individual material regions including conductor enamel and impregnation are represented in the model. Such model definition is usually realised by the use of finite element methods allowing for detailed representation of the machine complex geometrical features.

The layered winding representation, Fig. 1b), was developed to accelerate the thermal model setting-up and solving time while maintaining accuracy of the temperature predictions including the hot-spot identification [2, 8]. In this approach, the physical winding representation is transformed into the layered equivalent, such that the volumetric contribution of each of the individual winding materials remains unchanged. The number of model layers is chosen using an analytical formulae allowing for correct predictions for the hot-spot location [8]. The technique is well suited for the equivalent-circuit lumped-parameter thermal modelling approach with model complexity ranging from medium to high.

The equivalent material method for the winding region approximation, Fig. 1c), is intended for reduced-order equivalent-circuit lumped-parameter thermal analysis, where temperature distribution within the winding body is of lesser importance [9, 10]. As for the previous approach, the volumetric contribution of each of the individual winding material is identical to that from the physical winding. However, the individual materials form here distinctive homogenous regions arranged by combining smaller discrete sub-region present in the physical winding, Fig. 1c).

The homogenised winding representation, Fig. 1d), requires thermal data for the winding amalgam to be known prior to machine thermal model definition. The complete winding is represented here by a single region defined with composite material data [11]. The equivalent winding thermal data is derived using the existing methods, which include the analytical, numerical and experimental approaches [11]-[20]. Such winding representation is suitable for both the finite element and equivalent-circuit thermal analysis, significantly simplifying the model definition, and reducing solving time [11]-[13]. Also, the approach allows for the inhomogeneous/non-uniform winding loss distribution to be accounted for by simply subdividing the winding region into smaller sections, Fig. 1d), informed with appropriate winding loss share per section [3, 4].

It is important to note that a common issue associated with all the winding model representations discussed here, and thermal analysis in general, is the need for hardware calibration. This allows for various manufacture and assembly factors, which are frequently challenging or impossible to derive theoretically, to be experimentally informed. There are numerous experimental approaches used in calibration of the winding region discussed in the literature: starting from winding material samples [11]-[19], through stator-winding sub-assembly [3, 4, 11] and finishing with complete machine assembly testing [8]-[10]. The winding material sample testing is particularly useful when high fidelity thermal modelling is considered requiring more detailed and computationally efficient winding model definition, i.e. homogenised winding representation.

The existing theoretical homogenisation methods were initially developed in the context of two-component composite materials for the electromagnetic or optic applications [21]-[23], later adapted in the thermal analysis [24]. The two-component formulae neglect the conductor electrical insulation, which has been shown essential to account for, particularly for the winding constructions impregnated with high thermal conductivity encapsulants [12]. It is important to note that the existing analytical methods are focused on winding constructions utilising round conductors, where the equivalent thermal conductivity across the conductors is usually expected to be isotropic. This approximation however, is not valid for the windings formed with rectangular conductor or Litz wires, where the winding individual materials are distributed non-uniformly within the stator slot. The existing empirically derived data highlight the importance of accounting for the winding thermal anisotropy [13]-[18].

The other class of theoretical techniques used to estimate equivalent thermal properties for the homogenised winding region makes use of the finite element analysis. Here, to estimate the composite material properties a model representation emulating the winding material sample is employed [7, 12]. The technique has been shown suitable for winding constructions, where no lateral conductor transposition is present [7]. It is important to remind that all the homogenisation techniques discussed here refer to the equivalent thermal conductivity across the conductors only. The thermal conductivity along the conductors and specific heat capacitance can be derived from the volumetric share and thermal properties of the individual materials [12].

In this investigation two analytical methods for deriving equivalent thermal conductivity for the windings formed from rectangular conductors are proposed. The first one adapts the existing analytical homogenisation technique [12] by the use of a conductors stacking factor for both dimensional peripheries of the winding sample cross-section. The second method employs reduced-order equivalent-circuit lumped-parameters model representation for the winding amalgam. Both the proposed methods are informed by experimental data to account for the manufacture and assembly factors. The calibration approach used here is based on measured data from a single hardware material sample for a specific impregnation technique, conductor gauge, aspect ratio and fill factor to estimate the equivalent winding thermal conductivity for alternative conductor aspect ratios and fill factors. The proposed techniques have been discussed in details and demonstrated on a number of winding examples in successive sections of the paper. The theoretical predictions have been validated experimentally showing good correlation with the measured data.

2 Impregnated winding material samples

The manufacture and assembly nuances have a strong impact on the winding equivalent thermal conductivity [1, 2]. Consequently, the accurate estimation of the winding equivalent thermal conductivity requires a degree of hardware calibration. In this investigation a number of hardware samples of the impregnated windings have been manufactured using the techniques and materials commonly found in construction and assembly of electrical machines, Fig.2.

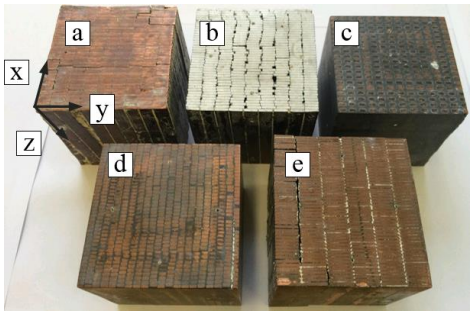

Figure 2: Impregnated winding samples with rectangular profiled conductors: aluminium (*Al*) conductors – Winding sample b, copper (*Cu*) conductors – Winding samples a, c, d and e

The former fully loaded with the conductors is then vacuum impregnated with an appropriate material. Here, two impregnating materials have been considered: solvent based varnish (Elmotherm 073-1010) and high thermal conductivity epoxy resin (Epoxylite EIP 4260). After the impregnation is cured, the former is removed, and the winding sample is machined to provide a 'good' surface finish required in measurements of the composite material thermal conductivity [11, 12]. The winding samples were selected here to differ in terms of conductor fill factor, material, aspect ratio, and impregnating material. All the conductors used in the sample manufacture are coated with the same grade of polyamide-imide enamel (class N) with thermal conductivity equal to 0.26W/(m·K) and measured thickness of 0.035mm per conductor side.

Winding sample	Conductor fill factor	Impregnating material	Conductor dimensions
a	75%	Varnish	(1.4×7.0=9.8) mm^2
b	77%	Varnish	(1.4×7.0=9.8) mm^2
c	27%	Epoxy	(1.5×3.0=4.5) mm^2
d	73%	Epoxy	(1.5×3.0=4.5) mm^2
e	77%	Varnish	(1.2×10.0=12.0) mm^2

Table 1: Basic data for the impregnated winding samples

The variety of the analysed samples enables a more generic insight into the composite winding thermal properties and their dependence on the geometrical, material and manufacture factors. Table 1 lists basic construction information for the analysed samples.

3 Experimental measurements

There are several experimental methods applicable in measuring of the equivalent thermal conductivity for composite materials. Some of which include the laser flash method [23] or the transient hot strip [24]. In this investigation the heat flux meter approach with cuboidal winding material samples has been employed [12]. The method emulates a unidirectional conductive heat transfer through a given axis of a winding material sample. It is assumed here that each of the sample axes is independent from each other. Due to conciseness, the theoretical fundamentals of the experimental method together with the testing procedure are not discussed in the paper. However, the authors' previous works provide comprehensive information addressing all these issues [11]-[13].

Winding sample	Thermal conductivity k_x [W/(m·K)]	Thermal conductivity k_y [W/(m·K)]	Conductor aspect ratio
a	2.0	2.2	5.0
b	1.9	2.0	5.0
c	2.0	2.3	2.0
d	4.0	4.3	2.0
e	1.9	3.1	8.3

Table 2: Measured set of thermal conductivities from tests on winding material samples together with conductors aspect ratio

Table 2 includes a set of measured thermal conductivities for each of the selected winding material samples supplemented with the conductor aspect ratio data. In the paper, the shorter dimension of the conductor cross-section is aligned with x-axis of the Cartesian coordinated system, Fig. 2, whereas the longer conductor cross-section periphery is alleged with y-axis. The experimental results suggest a degree of anisotropy for all the analysed winding samples. This is particularly prominent for the winding arrangements with relatively high conductor aspect ratio, Winding sample e. In general, the thermal conductivity in y-axis is larger than that in x-axis, which is attributed to the manner, in which the conductors are arranged.

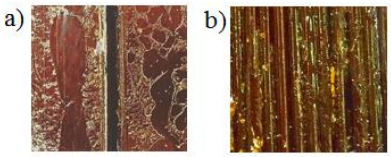

Figure 3: An example close-up on gaps between impregnated conductors for Winding sample e, a) x-axis, b) y-axis

Fig. 3 presents an example close-up on gaps between the individual conductors for the Winding version e revealing different gaps in x- and y-axis, larger for y-axis than x-axis. This partially explains lesser than expected impact of the conductor aspect ratio on the degree of anisotropy observed from the measurements. Also, the measured data indicates impact of the conductor fill factor on the equivalent winding thermal conductivity. A significant improvement is shown for windings with 'high' conductor fill factor as compared with counterparts with 'low' fill factor, Winding samples c and d. Furthermore, the use of epoxy resin impregnation has shown improved overall thermal properties of the impregnated winding samples. This results from better material thermal properties and improved encapsulating properties for the epoxy impregnation as compared with the varnish impregnation, where fill of the air pockets and cavities between conductors is usually poorer.

4 Mathematical models

Two methods of deriving equivalent thermal conductivity data for windings constructed with profiled rectangular conductors are discussed in this section. The first of the techniques adapts an existing analytical approach, whereas the second one makes use of reduced-order equivalent-circuit lumped parameter approach.

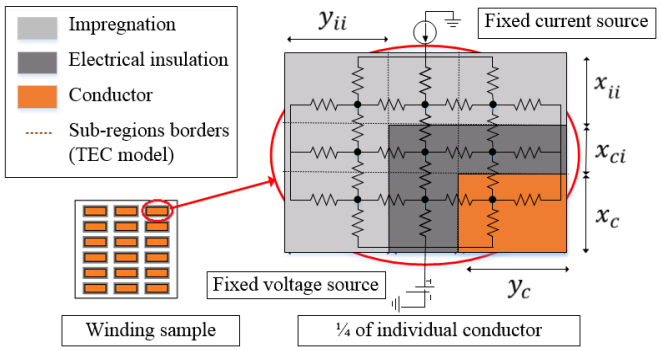

Figure 4: Schematic representation of the winding sample together with reduced-order equivalent-circuit lumped-parameter network representation and the nomenclature used

Fig. 4 presents schematic representation of the winding sample together with reduced-order equivalent-circuit model/ network representation and the nomenclature used. The subscripts *c*, *ci* and *ii* represent the conductor, conductor insulation/enamel and impregnation regions, respectively. The conductor electrical insulation thickness is assumed here to be identical for x- and y-axis of the material sample, $x_{ci} = y_{ci}$.

4.1 Proposed analytical method

The proposed analytical method is based on the Hashin and Shtrikman formula [23] altered by Simpson to account for three-material winding amalgam [12], which is further adapted in this paper to account for windings formed with rectangular conductors. The existing analytical expressions: Milton [21], Hashin and Shtrikman [23], Daniel and Corcolle [24] and Simpson [12] allow mainly for derivation of the equivalent thermal conductivity for composites constructed from two materials with stacked cylinders, round conductors and encapsulation.

$$k_e = k_a \frac{(1+v_c)k_c + (1-v_c)k_a}{(1-v_c)k_c + (1+v_c)k_a} \quad . (1)$$

Analytical expression for equivalent thermal conductivity, k_e, for two-component winding composite with round conductors is given by (1). Where: subscripts *c* and *a* refer to the conductor and electrical insulation/impregnation amalgam respectively. The material volume ratio v_c is taken to be equal to the conductor fill factor, $v_c = FF$. To account for three-material winding composite, (1) is adjusted with the following formula [12],

$$k_a = k_{ii} \frac{v_{ii}}{v_{ii} + v_{ci}} + k_{ci} \frac{v_{ci}}{v_{ii} + v_{ci}} \quad . (2)$$

In (2) volumetric ratio for each of the electrical insulation and impregnation regions is included. The volume ratio v_{ci} and v_{ii} is given as follows,

$$v_{ci} = v_c \frac{x_{ci}\,(x_c + y_c + x_{ci})}{x_c y_c} \quad . (3)$$

$$v_c + v_{ci} + v_{ii} = 1 \quad . (4)$$

The anisotropy of the winding is approximated here by the use of individual stacking factors for each of the x- and y-axes,

$$FF_x = \frac{x_c}{x_{ii} + x_{ci} + x_c}, FF_y = \frac{y_c}{y_{ii} + y_{ci} + y_c} \quad . (5)$$

The individual factors substitute *FF* when equivalent thermal conductivities k_x and k_y are estimated. However, this requires data regarding x_{ii} and y_{ii}, which is relatively simple to derive from the winding samples. It has been found from the measurements that for the analysed winding arrangements $x_{ii} = 0.48\, y_{ii}$ in average, further simplifying the proposed analytical method.

4.2 Proposed equivalent-circuit method

The proposed equivalent-circuit lumped-parameter approach of deriving equivalent thermal conductivity emulates the experimental method with heat flux meter and corresponds with the finite element model discussed in [12]. Fig. 4 presents the complete equivalent-circuit network with each of the winding material regions represented by four thermal resistances aligned with x and y winding axes. The common, central node for all the sets of resistors provides averaged temperature within the individual material regions. Such model definition stems from the fact of zero internal heat/power loss generation within the winding sample, i.e. heat is transferred across the winding sample only. Further to these, the model representation adopted in the analysis has been reduced to one quarter of an individual conductor including the enamel and impregnation regions. The initial analysis using the proposed approach and finite element analysis with complete and reduced-order models for the winding material samples have shown insignificant discrepancy between the results. The thermal conductivity in particular winding axis is derived from the heat rate, temperature difference across winding sample and geometrical dimensions [12, 13] by setting the fixed heat source and temperature boundary conditions across the axis. The remaining peripheries of the model are adiabatically insulated.

5 Results and observations

In order to demonstrate applicability and limitations of the proposed methods, the equivalent thermal conductivity for a number of winding topologies has been derived theoretically and experimentally. These have been supplemented with the finite element approach [12]. All the techniques: analytical, equivalent-circuit and finite element methods have been individually calibrated beforehand with experimental data from tests on the winding material samples.

Fig. 5 presents variation of the equivalent thermal conductivity in x- and y-axis, for the Winding sample e, versus conductor aspect ratio assuming fixed cross-section of an individual conductor and conductor fill factor. The results suggest an increase of k_y and decrease k_x for the conductor profiles with 'high' aspect ratios. All the analysed methods for deriving the equivalent thermal conductivity show similar

trends with some discrepancies towards 'small' conductor aspect ratios. Here, maximum deviation of 8% has been observed for both the analytical and equivalent circuit methods.

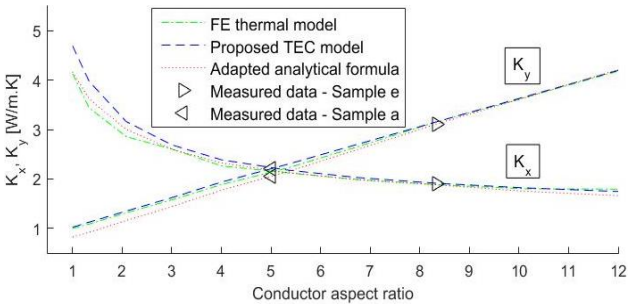

Figure 5: Thermal conductivity vs. conductor aspect ratio for varnish impregnated winding sample with copper conductors and *FF* = 77% – Winding sample e

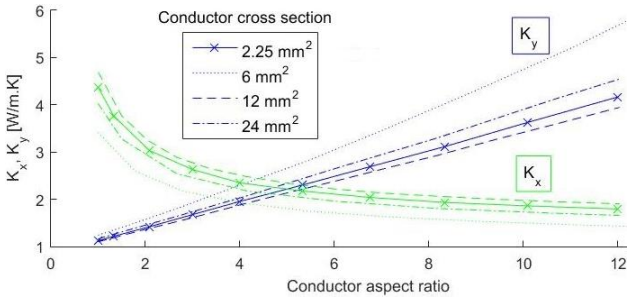

Figure 6: Thermal conductivity vs. conductor aspect ratio for varnish impregnated winding sample with copper conductors and *FF* = 77% and different conductor cross-section.

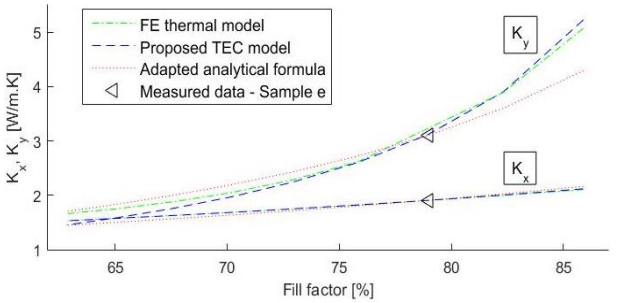

Figure 7: Thermal conductivity vs. conductor fill factor for varnish impregnated winding sample with copper conductors and conductor aspect ratio equal to 8.3 – Winding sample e

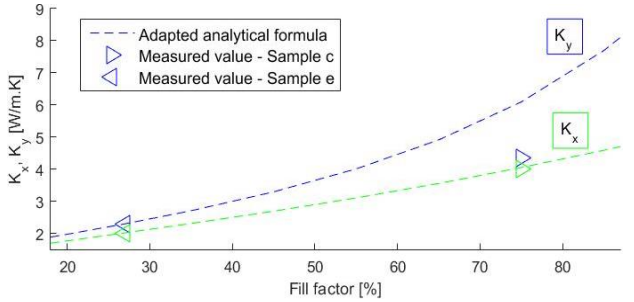

Figure 8: Thermal conductivity vs. conductor fill factor for epoxy impregnated winding sample with copper conductors and conductor aspect ratio equal to 2.0 – Winding samples c and d

It is important to note that for an ideal and symmetrical winding construction k_x and k_y are equal for the conductor aspect ratio equal to 1, i.e. conductor with square cross-section. However as it has been discussed earlier, stacking factors for both axes of the winding material samples are dissimilar and need to be derived from measurements. This different gapping between conductors in x and y axes shifts the $k_x = k_y$ point towards higher conductor aspect ratios, here equal to approximately 5. The results comparison shown in Fig. 5 assumes constant x- and y-axis stacking factors from the winding samples measurements.

An important element of the proposed techniques is hardware calibration with the reduced number of required material samples. In Fig. 5 measured data points for Winding versions a and e are included showing close correlation with the theoretical predictions. Both the material samples are constructed using the same conductor and varnish materials and have approximately the same conductor fill factor. The only difference between the samples lies in the conductor aspect ratio and conductor cross-section area. This suggests that winding hardware samples with similar constructions as outlined can be used to calibrate models with different conductor aspect ratios and conductor cross-section. This have been clearly illustrated in Fig. 6 where a number of theoretical winding examples with the same materials as for the Winding versions a and e, but different conductor-cross sections and conductor aspect ratios are compared. The theoretical findings suggest that the result transferability is limited and for conductor cross section more than 25% a new winding sample is required to calibrate the model.

Fig. 7 compares variation of the equivalent thermal conductivity with conductor fill factor. The theoretical predictions from all the analysed techniques show similar trends with data from the analytical method deviating from other techniques beyond 80% of the conductor fill factor. In particular, thermal conductivity in y-axis is affected with maximum discrepancy of 36% as compared with data from other methods. This limitation for the analytical method stems from simplified character of the approach where various volumetric and material measures are used to estimate the equivalent thermal conductivity. However, conductor fill factor beyond 80% are difficult to achieve for practical applications with profiled rectangular conductors.

Fig. 8 illustrates the effect of model calibration with experimental data from tests on material samples with different conductor fill factor, Winding samples c and d. It is important to note that the remaining construction factors are here identical, i.e. impregnation and conductor cross-section and aspect ratio. The models have been calibrated from hardware sample c to predict the equivalent thermal conductivity for winding sample d and vice versa. The results suggests that the model calibration with data, where conductor fill factors are significantly different, here 27% and 73%, does not allow for accurate predictions of the equivalent thermal conductivity.

6 Conclusion

The paper includes a detailed description of the proposed methods for deriving the equivalent thermal conductivity for impregnated windings formed with profiled rectangular

conductors accounting for the material thermal anisotropy. The techniques provide a building block for the high fidelity, computationally and resource effective thermal analysis. The theoretical background and practical use of the methods have been discussed in detail and demonstrated on a number of hardware examples providing an insight into applicability and limitation of the techniques. The calculated results from both the methods: analytical and equivalent circuit have shown good agreement with the finite element predictions and measured data.

The use of limited number of hardware winding samples has also been investigated. The results have shown that in cases of the winding samples constructed with the same materials/processes and similar winding factors it is possible to accurately predict the equivalent thermal conductivity for alternative windings with different conductor cross-section and/or conductor aspect ratio. When the conductor fill factor for the hardware sample and intended in the model are significantly different the model calibration approach with reduced winding samples has been shown to be inadequate.

Acknowledgements

The authors wish to thank the European Union for the funding to this research project (FP7 ITN Project 607361 ADEPT).

References

[1] A. Boglietti, A. Cavagnino, D. Staton, "Determination of critical parameters in electrical machine thermal models," *IEEE Trans. Ind. Appl.*, vol. 44, no. 4, pp. 1150–1159, Jul./Aug. 2008.

[2] D. Staton, A. Boglietti, A. Cavagnino, "Solving the more difficult aspects of electric motor thermal analysis in small and medium size industrial induction motors," *IEEE Trans. on Energy convers.*, vol. 20, no. 3, pp. 620–628, 2005.

[3] P. H. Mellor, R. Wrobel, N. Simpson, "AC losses in high frequency electrical machine windings formed from large section conductors," *IEEE Energy Conversion and Exposition, ECCE'2014,* pp. 1806-1813.

[4] R. Wrobel, D. Staton, R. Lock, J. Booker, D. Drury, "Winding design for minimum power loss and low-cost manufacture in application to fixed-speed PM generator," *IEEE Energy Conversion and Exposition, ECCE'2014*, pp. 5563-5570.

[5] L.J. Wu, Z.Q. Zhu, "Simplified Analytical Model and Investigation of Open-Circuit AC Winding Loss of Permanent Magnet machines," *IEEE Transactions on Industrial Electronics*, vol. 61, no. 9, pp.4990-4999, September 2014.

[6] L. Idoughi, X. Mininger, F. Bouillault, L. Bernard och a. E. Hoang, "Thermal model with winding homogenization and fit discretization for stator slot," *IEEE Trans. Magn.*, vol. 47, no. 12, pp. 4822-4826, 2011.

[7] A. Boglietti, A. Cavagnino, D. Staton, M. Shanel, M. Mueller, C. Mejuto, "Evolution and modern approaches for thermal analysis of electrical machines," *IEEE Trans. Ind. Electron.*, vol. 56, no. 3, pp. 871– 882, Mar. 2009.

[8] S. Nategh, O. Wallmark, M. Leksell, Z. Shuang, "Thermal analysis of a PMaSRM using partial FEA and lumped parameter modeling," *IEEE Trans. Energy Convers.*, vol. 27, no. 2, pp. 477–488, Jun. 2012.

[9] A. Boglietti, E. Carpaneto, M. Cossale, S. Vaschetto, M. Popescu, D. Staton, "Stator winding thermal conductivity evaluation: An industrial production assessment", *Energy Conversion Congress and Exposition ECCE'2015,* pp. 4865-4871.

[10] A. Boglietti, E. Carpaneto, M. Cossale, A. L. Borlera, D. Staton, M. Popescu, "Electrical machine first order short-time thermal transients model: Measurements and parameter evaluation," *Proc. Annu. Conf. IEEE Ind. Electron. Soc.*, 2014, pp. 555–561.

[11] R. Wrobel, P. H. Mellor, D. Holliday, "Thermal modelling of a segmented stator winding design*," IEEE Trans. Ind. Appl.*, vol. 47, no. 5, pp. 2023–2030, Sep./Oct. 2011.

[12] N. Simpson, R. Wrobel, P. H. Mellor, "`Estimation of Equivalent Thermal Parameters of Impregnated Electrical Windings,"' *IEEE Trans. on Industry Applications*, vol. 49, no. 6, pp. 25052515, Nov. 2013.

[13] R. Wrobel, P. Mellor, "A general cuboidal element for three-dimensional thermal modelling," *IEEE Trans. on Magnetics*, vol. 46, no. 8, pp. 3197–3200, 2010.

[14] R. Wrobel, A. Mlot, P. H. Mellor, "Contribution of end-winding proximity losses to temperature variation in electromagnetic devices," *IEEE Trans. Ind. Electron*., vol. 59, no. 2, pp. 848–857, Feb. 2012.

[15] R. Wrobel and P. H. Mellor, "Thermal design of high-energy-density wound components," *IEEE Trans. Ind. Electron*., vol. 58, no. 9, pp. 4096– 4104, Sep. 2011.

[16] R. Wrobel, S. Williamson, J. Booker, P. H. Mellor, "Characterising the performance of selected electrical machine insulation systems", *Energy Conversion Congress and Exposition, ECCE'2015*, pp.4857-4864.

[17] R. Wrobel, S.J. Williamson, N. Simpson, S. Ayat, J. Yon, P.H. Mellor, "Impact of slot shape on loss and thermal behaviour of open-slot modular stator windings", *Energy Conversion Congress and Exposition, ECCE'2015*, pp. 4433-4440.

[18] J. Baker, R. Wrobel, D. Drury. P. Mellor, "A Methodology for Predicting the Thermal Behaviour of Modular-Wound Electrical Machines", *IEEE Energy Conversion and Exposition, ECCE'2014*, pp. 5176 - 5183.

[19] R. Wrobel, D. Salt, N. Simpson, and P. H. Mellor, "Comparative study of copper and aluminium conductors - future cost effective PM machines," in *7th IET International Conference on Power Electronics, Machines and Drives, PEMD'2014*, pp. 16.

[20] L. Siesing, A. Reinap, M. Andersson, "Thermal properties on high fill factor electrical windings: Infiltrated vs non infiltrated," *Int. conf. in Electrical Machines, ICEM'2014*, pp. 2218–2223.

[21] G. W. Milton, "Bounds on the transport and optical properties of a two- component composite material," *Journal of Applied. Physique*., vol. 52, pp. 5294–5304, 1981.

[22] S. Torquato and F. Lado, "Bounds on the conductivity of a random array of cylinders*," Proc. R. Soc. Lond A 417*, pp. 59–80, 1988.

[23] Z. Hashin and S. Shtrikman, "A variational approach to the theory of the effective magnetic permeability of multiphase materials," *J. Appl. Phys.*, vol. 33, no. 10, pp. 3125–3131, Oct. 1962.

[24] L. Daniel and R. Corcolle, "A note on the effective magnetic permeability of polycrystals," *IEEE Trans. Magn*., vol. 43, no. 7, pp. 3153–3158, Jul. 2007.

[25] M. Jaritz and J. Biela, "Analytical model for the thermal resistance of windings consisting of solid or Litz wire," in *EPE 2013*, Lille, France, Sep. 3–5 2013.

[26] D. Lussier, S. Ormiston, R. Marko, "Theoretical determination of anisotropic effective thermal conductivity in transformer windings," *Int. Commun. Heat Mass Transfer*, vol. 30, no. 3, pp. 313–322, 2003.

[27] W. J. Parker, R. J. Jenkins, C. P. Butler, G. L. Abbott, "Flash method of determining thermal diffusivity, heat capacity, and thermal conductivity," *J. Appl. Phys.*, pp. 1679–1684, Sep. 1961.

[28] S. Gustafsson, "Transient hot strip techniques for measuring thermal conductivity and thermal diffusivity," *Rigaku J.*, vol. 4, no. 1/2, pp. 16–28, 1987.